Supplement of Hydrol. Earth Syst. Sci., 30, 2207–2223, 2026
https://doi.org/10.5194/hess-30-2207-2026-supplement

Hydrology and Earth System Sciences
Open Access
EGU

Supplement of

Adjusting diurnal error in dielectric-based in situ soil moisture measurements via Fourier time-filtering using land surface model datasets

Junnyeong Han et al.

Correspondence to: Eunkyo Seo (eseo@pknu.ac.kr)

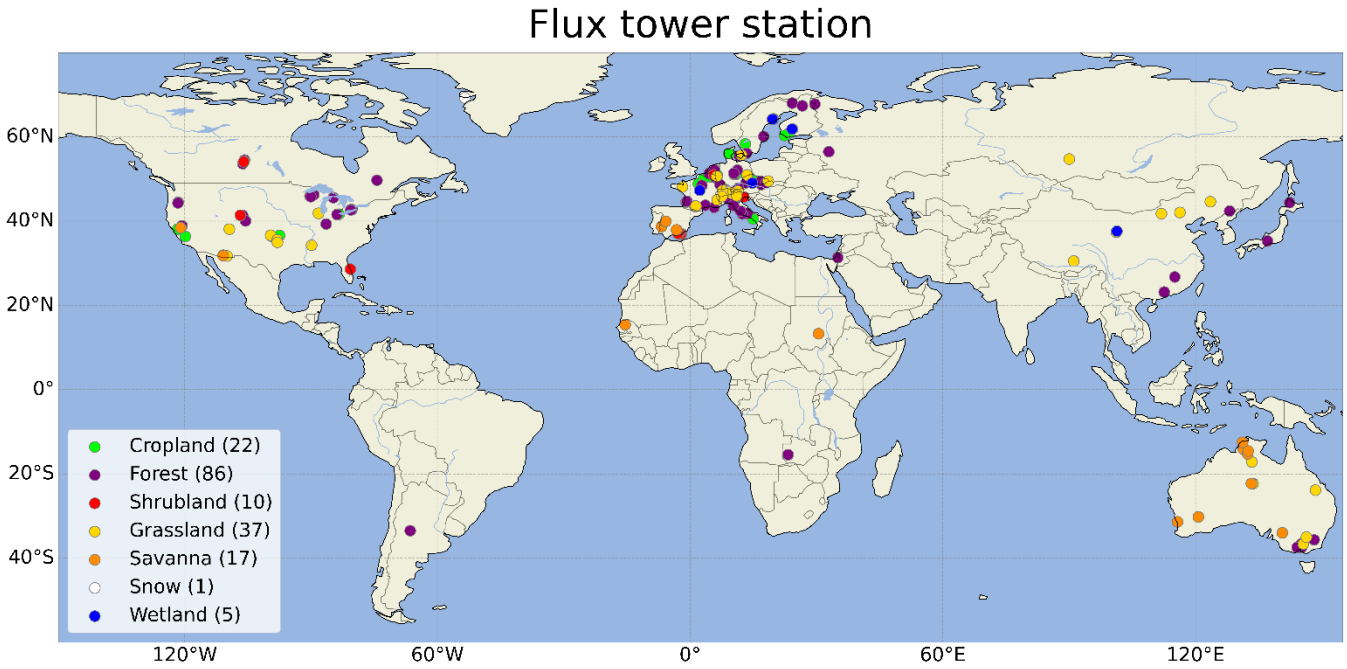

Figure S1: Spatial distribution of flux tower observation stations in Fig. 9, differentiated by IGBP land cover types.

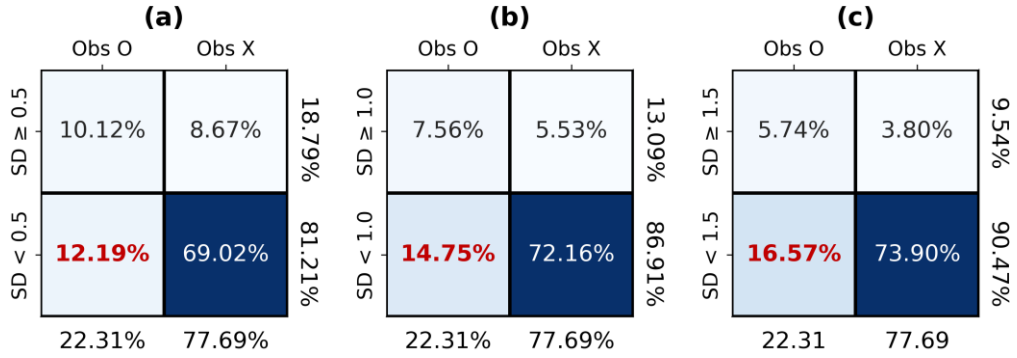

Figure S2: Contingency table comparing precipitation observations (Obs) and standard deviation (SD)-based removal classification using three SD thresholds: (a) 0.5, (b) 1.0, and (c) 1.5. "Obs O" and "Obs X" denote the presence and absence of observed precipitation, respectively. The y-axis indicates the SD-based removal result for each threshold. Values within each cell represent the percentage of total samples, while the marginal values at the bottom and right denote the column and row totals, respectively. The blue shading indicates the relative magnitude of the percentages, while the red bold values highlight cases where precipitation was observed but not removed by the SD-based method.

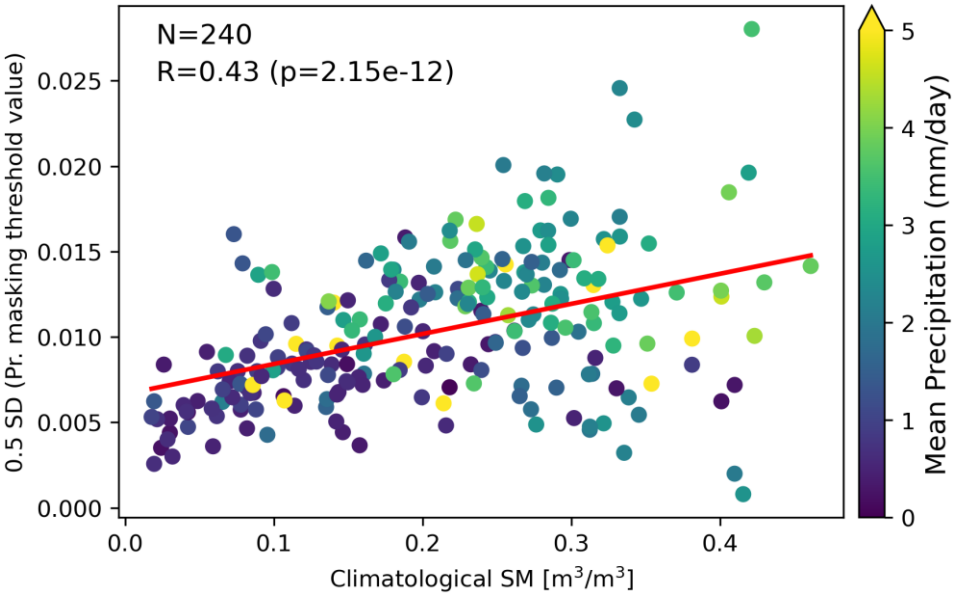

Figure S3: Scatter plot between climatological SM and the 0.5 SD precipitation-masking threshold across stations with observed precipitation (N=240), where shaded color in each dot indicates mean precipitation (mm/day). The correlation coefficient and its p-value are denoted in the upper-left corner.

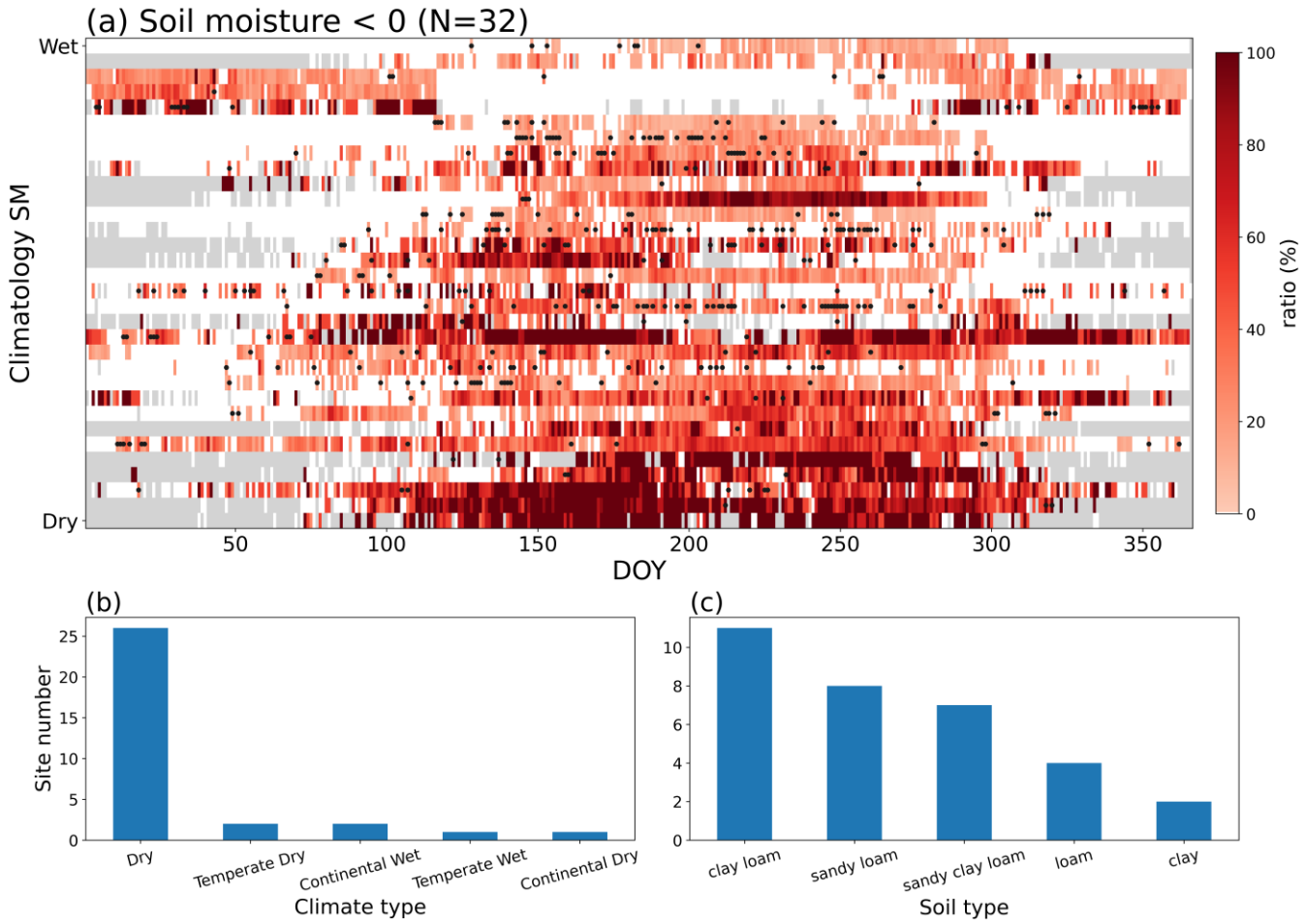

Figure S4: Stations (N=32) with more than 100 hours of negative SM values after the two-step adjustment. (a) Heatmap showing the ratio (%) of negative SM values averaged by Day of Year (DOY). The color scale represents the total fraction of negative SM occurrences after the adjustment. Black dots indicate negative SM values introduced during the diurnal mean correction, whereas colored areas without dots correspond to negative values generated during the FFT-based diurnal phase adjustment. Panel (b) and (c) show the distribution of these stations by climate type and soil type, respectively.

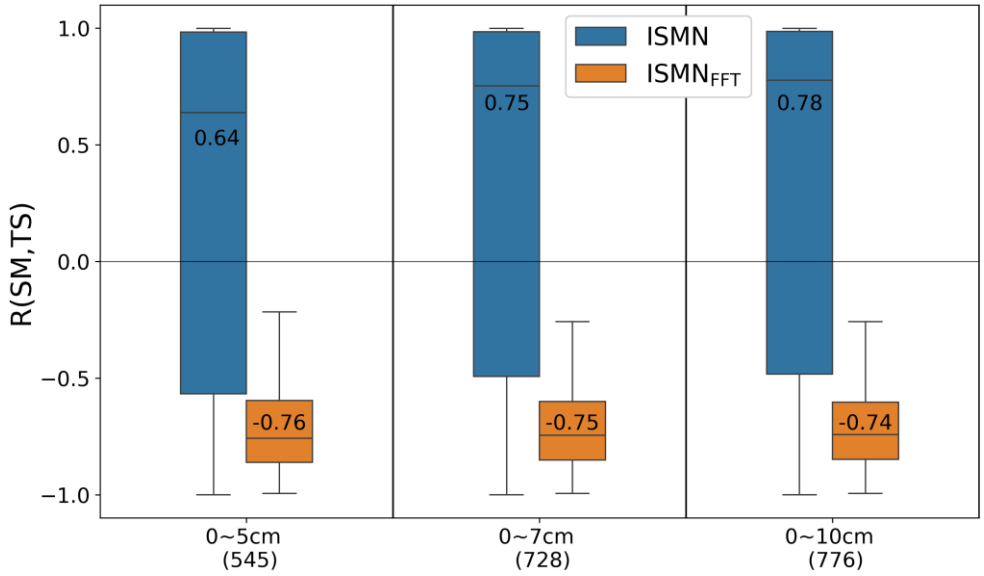

Figure S5: Boxplots of the diurnal correlation coefficient between SM and TS for the original time series (blue) and after adjustment (orange), grouped by observation depth by 0–5cm, 0–7cm, and 0–10cm. The values shown inside the boxes denote the median of the correlation coefficients at measurement sites. Numbers in parentheses (x-axis) indicate the number of stations at each grouped depth.

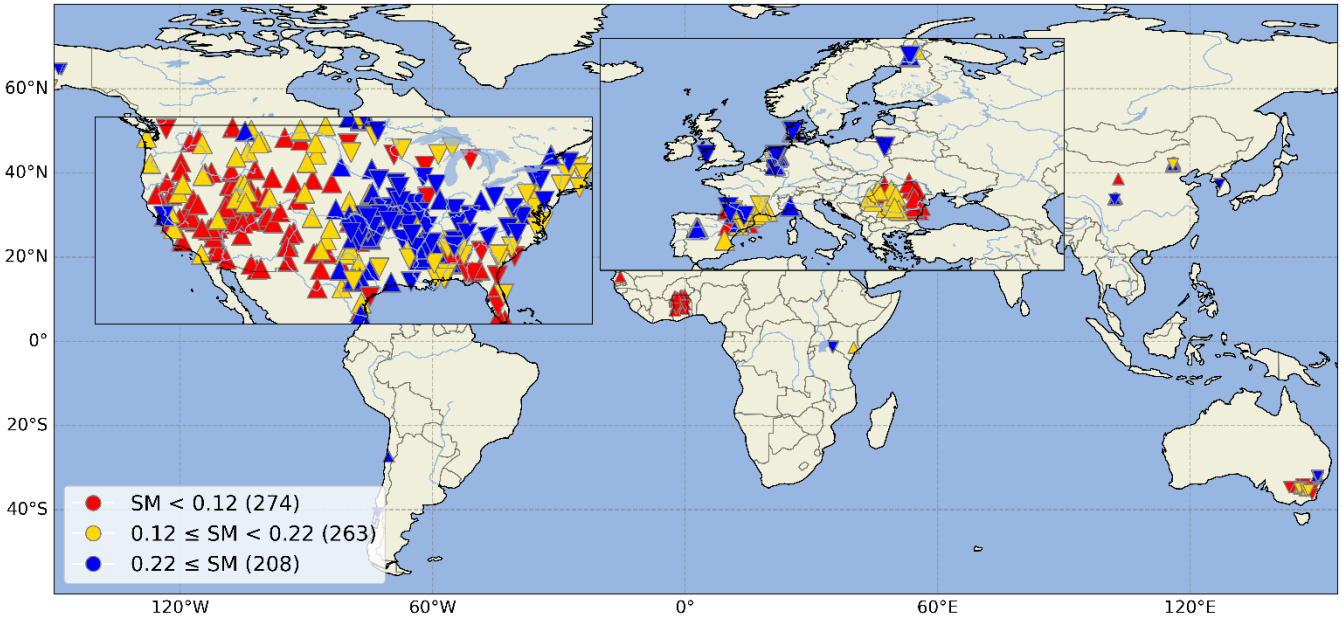

Figure S6: Spatial distribution of ISMN stations in Fig. 7a, classified with SM.

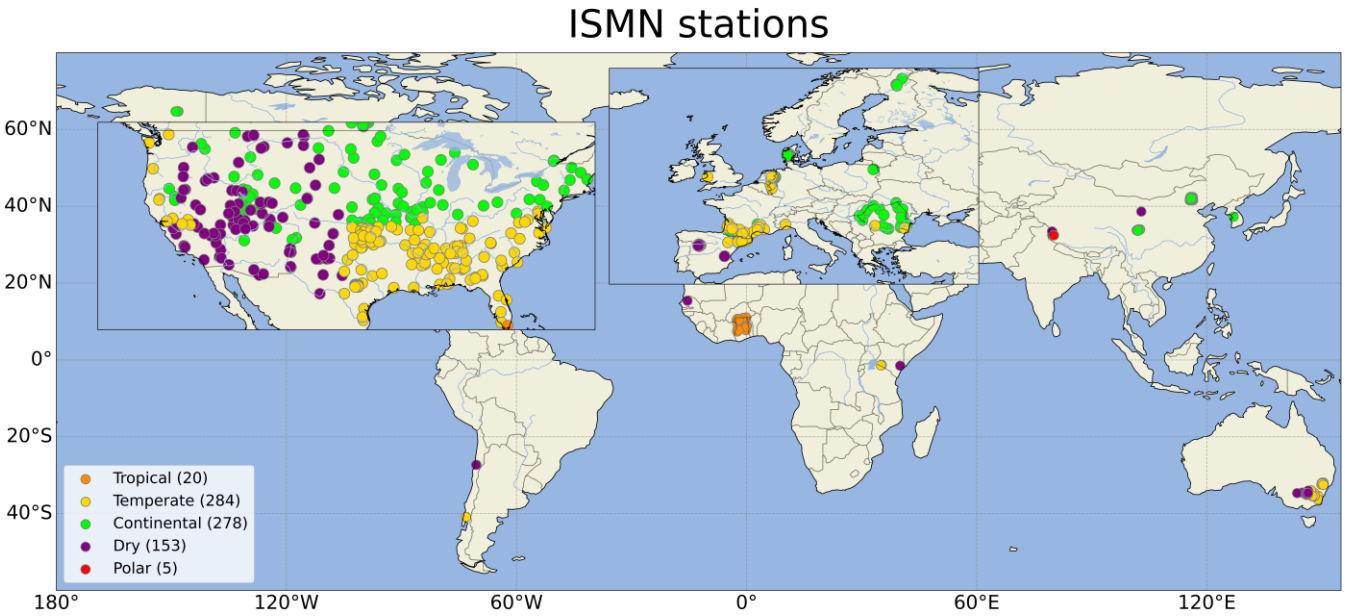

Figure S7: Locations of ISMN stations grouped according to the first-level Köppen-Geiger climate classification. Stations with unknown types (N=5) are not shown.

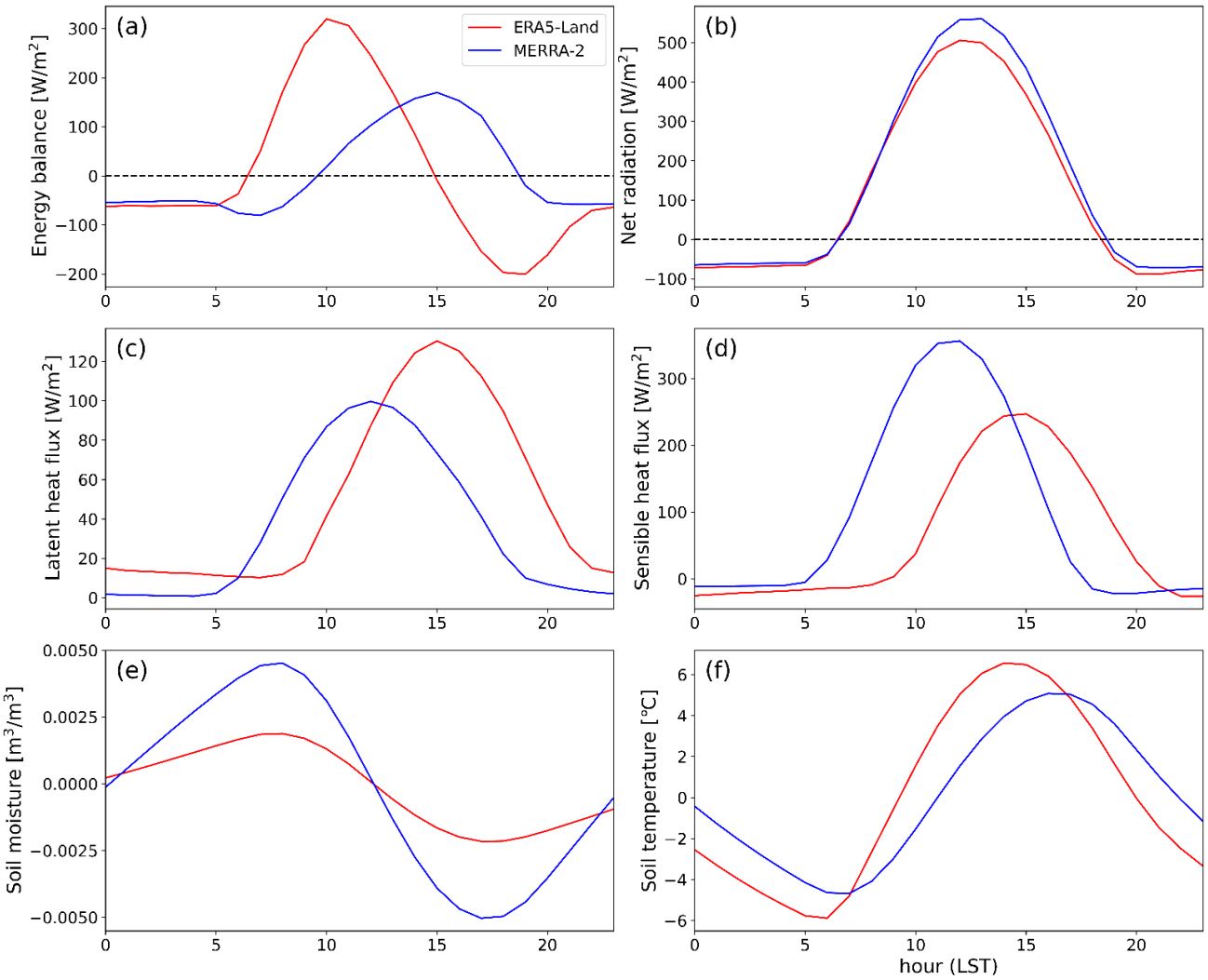

40 **Figure S8: Example of the diurnal cycle of (a) energy balance (SW_{net}+LW_{net}-LH-SH), (b) net radiation (SW_{net}+LW_{net}), (c) latent heat flux, (d) sensible heat flux, (e) surface SM, and (f) TS from ERA5-Land (red) and MERRA-2 (blue) at the RSMN-Calarasi station (44.21°N, 27.34°E).**

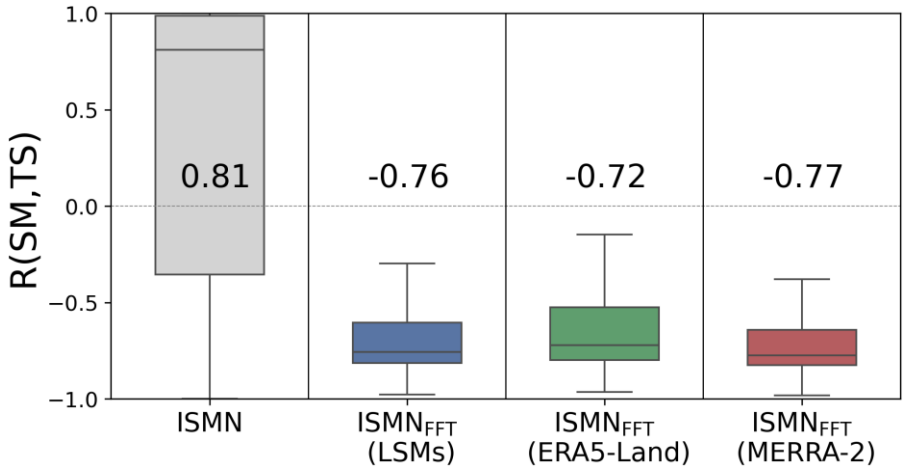

Figure S9: Boxplots of the diurnal correlation coefficient between SM and TS from ISMN, timely adjusted $ISMN_{FFT}$ using combined LSMs (ERA5-Land and MERRA-2), ERA5-Land only, and MERRA-2 only. Number in each cell indicates the median value of the correlation coefficients at measurement sites.